Fitoterapia 157 (2022) 105121

Contents lists available at ScienceDirect

Fitoterapia

journal homepage: www.elsevier.com/locate/fitote

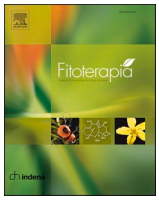

Biologically active polyphenolic compounds from *Lespedeza bicolor*

Darya V. Tarbeeva [a,*], Natalya V. Krylova [b], Olga V. Iunikhina [b], Galina N. Likhatskaya [a], Anatoliy I. Kalinovskiy [a], Valeria P. Grigorchuk [c], Mikhail Yu. Shchelkanov [b], Sergey A. Fedoreyev [a]

[a] G.B. Elyakov Pacific Institute of Bioorganic Chemistry, Far Eastern Branch, Russian Academy of Sciences, 690022 Vladivostok, Russia
[b] G.P. Somov Institute of Epidemiology and Microbiology, Rospotrebnadzor, 690087 Vladivostok, Russia
[c] Federal Scientific Center of the East Asia Terrestrial Biodiversity (Institute of Biology and Soil Science), Far Eastern Branch, Russian Academy of Sciences, 690022 Vladivostok, Russia

ARTICLE INFO

Keywords:
Herpes simplex virus type 1
Polyphenolic compounds
Antiviral activity

ABSTRACT

We investigated the ability of six prenylated prerocarpans, stilbenoid, and a new dimeric flavonoid, lespebicolin B, from stem bark as well as two 3-*O*-rutinosides and a mixture of 3-*O*-β-D-glucosides of quercetin and kaempferol from flowers of *Lespedeza bicolor* to inhibit HSV-1 replication in Vero cells. Pretreatment of HSV-1 with polyphenolic compounds (direct virucidal effect) showed that pterocarpans lespedezol A_2 (**1**), (6a*R*,11a*R*)-6a,11a-dihydrolespedezol A_2 (**2**), (6a*R*,11a*R*)-2-isoprenyldihydrolespedezol A_2 (**4**), and (6a*R*,11a*R*,3'*R*)-dihydrolespedezol A_3 (**5**) significantly inhibited viral replication, with a selective index (SI) ≥10. Compound **4** possessed the lowest 50% – inhibiting concentration (IC_{50}) and the highest SI values (2.6 μM and 27.9, respectively) in this test. (6a*R*,11a*R*)-2-Isoprenyldihydrolespedezol A_2 (**4**) also had a moderate effect under simultaneous treatment of Vero cells with the tested compound and virus (IC_{50} and SI values were 5.86 μM and 12.4, respectively). 3-*O*-rutinosides of quercetin and kaempferol and a mixture of 3-*O*-β-D-glucosides of quercetin and kaempferol (**10** and **12**) also showed significant virucidal activity, with SI values of 12.5, 14.6, and 98.2, respectively, and IC_{50} values of 8.6, 12.2, and 3.6, respectively.

We also performed a quantitative structure–activity relationship (QSAR) analysis of data on the virucidal activity of polyphenolics with $4 < pIC_{50} < 6$. It was found that the virucidal activity of these compounds depended on both the structure of the aromatic part and the conformation of geranyl and isoprenyl side chains of their molecules. These findings are correlated with the largest value of the principal moment of inertia (pmi) descriptor describing the geometry of molecules.

1. Introduction

Lespedeza bicolor Turcz is a shrub plant belonging to the Leguminosae family. *L. bicolor* extracts possess a wide spectrum of biological activity: antioxidant, anti-inflammatory, estrogenic, antimicrobial, antifungal [1–4], antitumor, and antityrosinase activities [5,6]. *L. bicolor* extract was shown to reduce methylglypxal-induced glucotoxicity in vitro and in vivo [7–9] and to possess a potent memory-enhancing effect [10].

L. bicolor shoots contain sufficient amounts of widespread flavonoids (quercetin, kaempferol, quercetin 3-*O*-glucoside (isoquercitrin), homoorientin, orientin, eriodictyol), isoflavonoid (daidzein), chalcon (isoliquiritigenin), and hydroxybenzoic acids (caffeic and protocatechuic), whereas the polyphenolic composition of *L. bicolor* root and stem bark is significantly different, with the most abundant class of polyphenolics being the rarer prenylated pterocarpans [7,10–17]. Several prenylated polyphenolic compounds have been previously isolated from *L. bicolor* roots and are able to inhibit bacterial neuraminidase activity [13]. Prenylated pterocarpans have also been shown to inhibit the growth of human prostate cancer, triple-negative breast cancer, and blood cancer cells via various mechanisms [14–17]. However, it is important to note that prenylated polyphenolic compounds from *L. bicolor* have not been tested for their antiviral activity, including antiherpetic properties, so far.

Herpetic infections are a group of the most common and poorly controlled human infections, which occur in the form of latent subclinical and clinically manifest forms caused by herpes simplex viruses

* Corresponding author.
E-mail address: tarbeeva1988@mail.ru (D.V. Tarbeeva).

https://doi.org/10.1016/j.fitote.2021.105121
Received 31 October 2021; Received in revised form 27 December 2021; Accepted 28 December 2021
Available online 3 January 2022

(HSVs) [18]. Herpes simplex virus type 1 (HSV-1) is a DNA-containing virus of the Herpesviridae family of the Alphaherpesvirinae subfamily that causes orofacial herpes. This virus causes human infectious diseases of varying severity, from characteristic vesicular rashes coming out on skin to lesions of the central nervous system. The severity of complications and the emergence of drug resistance make herpes infection a global health problem [19,20]. In a body with a normal immune system, herpes viruses can circulate asymptomatically, but in people with immunosuppression they cause serious and fatal illnesses. According to the World Health Organization, infections caused by HSV are the third most widespread viral diseases in humans after COVID-19 and influenza [21,22]. The only clinically approved antiherpetic drugs for the treatment of HSV-1 infection so far are acyclovir and its analogs, which are inhibitors of viral DNA replication [23,24]. However, the emergence of resistant viral strains has encouraged the search for new antiherpetic alternatives [25–27].

Today, many reports are emerging on the antiviral activity of plant extracts, individual flavonoids, and related polyphenolic compounds [28,29]. However, nothing is known so far about the antiherpetic properties of polyphenolic compounds from *Lespedeza* genus plants.

Here, we studied the antiviral activity of polyphenolic compounds from *L. bicolor* stem bark and flowers against HSV-1 infection and performed a QSAR analysis of data on their virucidal activity.

2. Materials and methods

2.1. Plant material

L. bicolor was collected in Khasansky District (Andreevka village) of the Primorye Region (The Russian Federation) from a grassy dry meadow in August 2016 by academician P.G. Grovoy. Voucher specimen No. 103608 was kept in the herbarium of the Laboratory of Chemotaxonomy (G.B. Elyakov Pacific Institute of Bioorganic Chemistry, FEB RAS).

2.2. Extraction and isolation

Pterocarpans **1–7** and stilbenoids **7** were isolated as described in our previous papers [14,15]. In order to isolate dimeric flavonoid **8**, the air-dried stem bark of *L. bicolor* (200 g) was extracted twice under reflux with a $CHCl_3$–EtOH mixture at a volume ratio of 3:1 for 3 h (60 °C). The obtained extract of *L. bicolor* stem bark (2.2 g) was chromatographed on a polyamide column (90 g, 50–160 μm, Sigma-Aldrich, St. Louis, MO, USA). The column was eluted with a hexane–$CHCl_3$ solution system with gradually increasing $CHCl_3$ amounts (hexane/$CHCl_3$, 1:0, 100:1, 50:1, 40:1, *v/v*) to give fractions 1–14 and then with a $CHCl_3$–EtOH solution system with gradually increasing EtOH amounts ($CHCl_3$/EtOH, 1:0, 100:1, 50:1, 40:1, *v/v*) to give fractions 15–22. Fraction 21 (307 mg), eluted with $CHCl_3$–EtOH (20:1), was also chromatographed on a silica gel column using the same solution system to obtain compound **8** (14.5 mg). Compound **8** was eventually purified using the preparative HPLC technique.

Air-dried flowers of *L. bicolor* (200 g) were extracted twice under reflux with a $CHCl_3$–EtOH mixture at a volume ratio of 3:1 for 3 h (60 °C). The obtained extract of *L. bicolor* flowers (1.4 g) was chromatographed on a polyamide column (90 g, 50–160 μm, Sigma-Aldrich, St. Louis, MO, USA). The column was eluted with a $CHCl_3$–EtOH solution system with gradually increasing EtOH amounts ($CHCl_3$/EtOH, 1:0, 100:1, 50:1, 40:1, *v/v*) to give fractions 1–18. The fractions containing polyphenolic compounds according to HPLC data were further purified. Fraction 11 was chromatographed on a Toyopearl HW-50 column (Sigma-Aldrich, St. Louis, MO, USA) to give fractions **10**, **11**, and **22** eluted with 20%, 25%, and 65% aqueous ethanol solution, respectively. These fractions were subsequently purified on a C-18 column (Sigma-Aldrich, St. Louis, MO, USA) to give compounds **9** and**11** and a mixture of compounds **10** and **12**, respectively.

*Lespebicolin B (**8**):* Yellow, amorphous powder;$[\alpha]_{Hal}^{20}$ – 99 (1 mg/mL, MeOH); UV (MeOH), λ_{max} 206, 270, 318 nm; CD (4.55 × 10^{-4} M, CH_3CN) λ_{max} (θ) 198 (+28,977), 214 (−45,398), 236 (−19,273), 272 (−5187), 300 (−3947), 340 (−8925), 395 (+1841); ^1H and ^{13}C NMR data, see Table 1; HR-ESI-MS *m/z*879.4072 [M–H] (calcd for $[C_{55}H_{59}O_{10}]^-$ 879.4113,), *m/z*881.4241 [M + H] + (calcd for $[C_{55}H_{61}O_{10}]^+$ 881.4259).

2.3. Analytical and preparative HPLC

The analytical HPLC was carried out using an Agilent Technologies 1260 Infinity II HPLC system (Agilent Technologies, Waldbronn, Germany) equipped with a VWD detector (λ = 280 nm). The extracts and fractions were analyzed using a Supelco Analytical HS-C18 (Supelco Analytical, Bellefonte, PA, USA) column (3 μm, 4.6, 75 mm) thermostated at 30 °C. The mobile phase consisted of 1% aqueous acetic acid (A) and acetonitrile containing 1% acetic acid (B). For the analysis, the following gradient steps were programmed: 0–2 min, 5% B; 2–4 min, 5–20% B; 5–17 min, 20–50% B; 18–23 min, 50–90% B; 24–25 min, 90–100% B; 16–27 min, 100% B; 28–33 min, 100–5% B. The flow rate was 0.8 mL/min. The data were analyzed with OpenLab CDC software v. 2.4 (Agilent Technologies, Waldbronn, Germany).

The preparative HPLC was carried out using a Shimadzu HPLC system equipped with an LC-20AT pump and SPD-20A detector (λ = 280 nm) (Shimadzu, Kyoto, Japan). The polyphenolic compounds were purified using a silicagel YMC-Pack SIL (Supelco Analytical, Bellefonte, PA, USA) column (5 μm, 10, 250 mm). The mobile phase consisted of hexane (97%) and isopropanol (3%). The flow rate was 4.5 mL/min. The data were acquired and processed using Shimadzu LCMS Solution software (v. 5.93, Shimadzu, Kyoto, Japan).

2.4. HR-ESI-MS

HR-ESI-MS experiments were performed using a Shimadzu hybrid ion trap–time-of-flight mass spectrometer (Shimadzu, Kyoto, Japan). We applied the following operating settings for the instrument: electrospray ionization (ESI) source potential, 3.8 and 4.5 kV for negative and positive ion mode, respectively; drying gas (N_2) pressure, 200 kPa; nebulizer gas (N_2) flow, 1.5 L/min; temperature for the curved desolvation line (CDL) and heat block, 200 °C; detector voltage, 1.5 kV; range of detection, 100–900 *m/z*. The mass accuracy was below 4 ppm. The data were acquired and processed using Shimadzu LCMS Solution software (v.3.60.361, Shimadzu, Kyoto, Japan).

2.5. Virus and cell culture

Herpes simplex virus type 1 (HSV-1) strain L2 was obtained from N. F. Gamaleya Federal Research Centre for Epidemiology and Microbiology (Moscow, Russia). HSV-1 was grown in African green monkey kidney cells (Vero) using Dulbecco's Modified Eagle's Medium (DMEM) supplemented with 10% fetal bovine sera (FBS) and 100 U/mL of gentamycin at 37 °C in a CO_2 incubator. The FBS concentration in the maintenance medium was decreased to 1%.

2.6. Cytotoxicity of polyphenolic compounds

The cytotoxicity of polyphenolic compounds was estimated by the MTT assay in Vero cells [30]. Cell monolayers (1 × 10^4 cells/well) in 96-well plates were treated with different concentrations of polyphenolic compounds (from 0.2 to 1000 μM) and incubated at 37 °C in a CO_2 incubator for 72 h. Untreated cells were used as controls. MTT solution (methylthiazolyltetrazolium bromide, Sigma, USA) was added to cells at a concentration of 5 mg/mL, and then the cells were incubated for 2 h at 37 °C. After dissolution of formazan crystals, the optical density was measured at 540 nm (Labsystems Multiskan RC, Vantaa, Finland).

Table 1
^{1}H (700 MHz), ^{13}C (175 MHz), HMBC, COSY, and ROESY NMR data for compound **8** (δ in ppm, J in Hz, $CDCl_3$). The carbon atoms marked with an asteric may be reversable.

	^{13}C	^{1}H	HMBC	COSY	ROESY
Upper moiety (I)					
2	154.0	–	–	–	–
3	119.5	–	–	–	–
4	194.5	–	–	–	–
5	103.5	6.81, s, 1H	C-6, 7, 9, 10	–	–
6	141.9	–	–	–	–
7	147.4	–	–	–	–
8	111.0	–	–	–	–
9	141.5	–	–	–	–
10	117.90	–	–	–	–
1′	110.8	–	–	–	–
2′	156.4	–	–	–	–
3′	105.0	6.50, d, J = 2.4, 1H	C-1′, 2′, 4′, 5′	–	–
4′	158.6	–	–	–	–
5′	108.6	6.41, dd, J = 2.4, 8.4, 1H	C-1′, 3′	H-6	–
6′	132.2	7.25, d, J = 8.4, 1H	C-2, 2′, 4′	H-5	–
1″	23.4	3.69, d, J = 7.4, 2H	C-7, 8, 9, 2″, 3″, 4″ (weak), 5″ (weak)	H-2″, 4″, 9″	H-2″, 9″
2″	120.4	5.42, t, J = 7.2, 1H	C-8, 1″, 4″, 9″	H-1″, 4″, 9″	H-1″, 4″
3″	139.3	–	–	–	–
4″	39.7	2.10, m, 2H	C-2″, 3″, 5″, 6″, 9″	H-1″, 2″, 5″	H-2″
5″	26.4	2.13 m, 2H	C-3″, 4″, 6″, 7″	H-4″, 6″, 8″, 10″	–
6″	123.8	5.07, m, 1H	C-4″, 8″, 10″	H-5″, 8″, 10″	–
7″	132.1	–	–	–	–
8″	25.7	1.67, s, 3H	C-4″ (weak), 6″, 7″, 10″	H-5″, 6″	–
9″	16.3	1.86, s, 3H	C-2″, 3″, 4″	H-1″, 2″	H-1″
10″	17.7	1.60, s, 3H	C-6″, 7″, 8″	H-5″, 6″	–
OH-7		5.78, s, 1H	C-6 (weak), 8 (weak)	–	OH-6
OH-6		5.27, bs, 1H	–	–	OH-7
Lower moiety (II)					
1	132.0	7.21, s, 1H	C-3, C-4, C-4a, C-11a, C-1‴″	H-1‴″	H-1‴″, 11a
2	121.5	–	–	–	–
3	155.9	–	–	–	–
4a	154.9	–	–	–	–
4b	103.9	6.36, s, 1H	C-2, 3, 4a, 11a (weak), 11b,	–	–
6	69.3	3.57, m, 1H 3.99, m, 1H	– –	–	–
6a	39.4	3.45, m, 1H	–	H-11a	–
6b	118.5	–	–	–	–
7	127.2	7.34, s, 1H	C-4 (upper), 9, 10a	–	–
8	113.3	–	–	–	–
9	164.8*	–	–	–	–
10	112.1	–	–	–	–
10a	164.9*	–	–	–	–
11a	79.3	5.57, d, J = 7.0, 1H	C-4a	H-6a	H-1
11b	112.2	–	–	–	–
1‴	22.2	3.32, m, 2H	C-2‴, 3‴, 9, 10, 10a	H-2‴, 9‴	H-2‴, 9‴
2‴	121.0	5.25, m, 1H	C-10, 1‴, 4‴, 9‴	H-1‴, 4‴, 9‴	H-1‴, 4‴
3‴	135.9	–	–	–	–
4‴	39.8	1.97, m, 2H	C-2‴, 3‴, 5‴, 6‴, 9‴	H-2‴	H-2‴
5‴	26.7	2.05, m, 2H	C-3‴, 4‴, 6‴,7‴	H-6‴, 8‴, 10‴	–
6‴	124.4	5.07, m, 1H	C-4‴, 8‴, 10‴	H-5‴, 8‴, 10‴	–
7‴	131.3	–	–	–	–
8‴	25.7	1.64, s, 3H		H-5‴, 6‴	–
9‴	16.1	1.78, s, 3H	C-4‴(weak), 6‴, 7‴, 10‴ C-2‴, 3‴, 4‴	H-1‴, 2‴	H-1‴
10‴	17.7	1.57, s, 3H	C-6‴, 7‴, 8‴	H-5‴, 6‴	–
1⁗	29.2	3.33, m, 2H	C-1, 2, 3, 2⁗, 3⁗, 5⁗(weak)	H-1, 2⁗	H-1, 2⁗
2⁗	121.6	5.32, t, J = 7.6, 1H	C-2, 1⁗, 4⁗, 5⁗	H-1⁗, 4⁗, 5⁗	H-1⁗
3⁗	135.2	–	–	–	–
4⁗	25.8	1.79, s, 3H	C-2⁗, 3⁗, 5⁗	H-2⁗	–
5⁗	17.9	1.79, s, 3H	C-2⁗, 3⁗, 4⁗	H-2⁗	–
OH-9		12.83, bs, 1H	–	–	–

Cytotoxicity was expressed as the 50% cytotoxic concentration (CC_{50}) of each studied compound that reduced the viability of treated cells by 50% compared to untreated cells and was calculated using regression-analysis-generated data from three independent experiments [31].

2.7. Anti-HSV-1 activity of the tested compounds

The antiviral activity of polyphenolic compounds against HSV-1 was evaluated using the CPE inhibition assay in Vero cells. The monolayers of Vero cells grown in 96-well plates (1×10^4 cells/well) were infected with 100 $TCID_{50}$/mL (the 50% tissue culture infectious dose) of HSV-1. Four schemes of the treatment of cells or virus with polyphenolic compounds (0.2–100 μM) were applied. The plates were incubated at 37 °C in a CO_2 incubator for 72 h until 80–90% CPE was observed in the virus control compared with the cell control. Each experiment was repeated trice.

2.7.1. Pretreatment of virus with polyphenolic compounds

An infectious dose of virus (100 $TCID_{50}$/mL) was mixed with different concentrations of studied compounds in a ratio 1:1 (*v*/v) and incubated for 1 h at 37 °C.Then, the mixture was applied to the cell monolayer. After 1 h of adsorption at 37 °C, the cells were washed with phosphate-buffered saline (PBS), overlaid by the maintenance medium, and incubated until CPE was observed.

2.7.2. Pretreatment of cells with polyphenolic compounds

The monolayer of cells was pretreated with different concentrations of studied compounds for 2 h at 37 °C. After washing, the cells were infected with 100 $TCID_{50}$/mL of HSV-1 at 37 °C for 1 h. Then, unabsorbed virus was removed by washing with PBS, and cells were incubated in the maintenance medium until CPE appeared.

2.7.3. Simultaneous treatment of the cells with polyphenolic compounds and virus

The monolayer of cells was infected with the virus (100 $TCID_{50}$/mL) and simultaneously treated with different concentrations of the studied polyphenolic compounds (virus/compound, 1:1 *v*/v) for 1 h at 37 °C. After virus adsorption, the mixture was removed, and the cells were washed with PBS and incubated in maintenance medium until CPE appeared.

2.7.4. Treatment of virus-infected cells with polyphenolic compounds

The monolayer of cells was infected with 100 $TCID_{50}$/mL of HSV-1 at 37 °C for 1 h, and then the cells were washed with PBS and treated with different concentrations of the studied compounds and incubated before apparent CPE appeared.

After incubation, the cell supernatants were collected, and virus titers were calculated using the Reed-Muench method [32] and expressed as $TCID_{50}$/mL. The antiviral effect of polyphenolic compounds was determined by the difference in viral titers between the treated infected cells and the untreated infected cells and expressed as the virus

inhibition rate (IR, %). The IR was calculated according to the following formula: IR = (1 − T/C) × 100%, where T is the antilog of the compound-treated viral titers, and C is the antilog of the control (without compound) viral titers [32]. IC_{50} of each compound was determined as the compound concentration that inhibited virus-mediated CPE by 50% and was calculated using a regression analysis [33]. SI was calculated as the ratio of CC_{50} to IC_{50} for each compound.

2.8. Computer modeling and QSAR

In the present study, a dataset of 5 compounds from Table 2 and 4 compounds from Table 3 were used for 3D-structure modeling and optimization with the Amber10:EHT force field using the Build module of the MOE 2020.0901 program [34]. The dataset was used for descriptor calculations with the QuaSAR module of MOE 2020.0901. The EC_{50} values were converted into corresponding pIC_{50} values ($-\log IC_{50}$) to be included in the database. The pIC_{50} values determined in this work for 9 compounds with $4 < pIC_{50} < 6$ were added to the database with the structures of the studied compounds. The dataset of the 9 compounds with $4 < pIC_{50} < 6$ was used for the generation of a QSAR model and its validation.

3. Results and discussion

3.1. Polyphenolic compounds of L. bicolor stem bark

We isolated six previously published compounds [pterocarpen lespedezol A_2 (**1**), prerocarpans (6a*R*,11a*R*)-6a,11a-dihydrolespedezol A_2 (**2**), (6a*R*,11a*R*)-8-*O*-methyl-6a,11a-dihydrolespedezol A_2 (**3**), (6a*R*,11a*R*)-2-isoprenyldihydrolespedezol A_2 (**4**), (6a*R*,11a*R*,3'*R*)-dihydrolespedezol A_3 (**5**), (6a*R*,11a*R*,3'*S*)-dihydrolespedezol A_3 (**6**), stilbenoid bicoloketone (**7**)] and a new dimeric flavonoid (**8**) from *L. bicolor* stem bark (Fig. 1). In order to perform structural identification of pterocarpans **1–6** and stilbenoid **7**, we compared their ^1H and ^{13}C NMR spectra with the spectra obtained for these compounds in our previous studies [14,15].

Compound **8** was obtained as a yellow amorphous powder. Its HR-ESI-MS spectrum contained the $[M + H]^+$ ion at *m/z* 881.4241 in the positive ion mode (calc. 881.4259 for $[C_{55}H_{61}O_{10}]^+$) and the $[M–H]^-$ ion at *m/z* 879.4072 (calc. 879.4113 for $[C_{55}H_{59}O_{10}]^-$) in the negative ion mode. Thus, the molecular formula of **8** was determined to be $C_{55}H_{60}O_{10}$ (Figs. S1 and S3, Supplementary data). The presence of the 2-arylbenzofuran (upper moiety, I) and pterocarpan (lower moiety, II) fragments, linked with the carbonyl group, was confirmed using the tandem mass spectrometry technique. The negative MS/MS product ions at *m/z* 419.1484 with the composition $[C_{25}H_{23}O_6]^-$ (calc. 419.1500) and at *m/z* 393.1696 with the composition $[C_{24}H_{25}O_5]^-$ (calc. 393.1707) resulted from carbonyl bridge degradation and indicated a neutral loss of a pterocarpan fragment (II) (Fig. S4, Supplementary data). The signal at *m/z* 487.2473 (calc. 487.2479) in the positive ion mode corresponded to the ion $[C_{31}H_{35}O_5]^+$ and indicated the loss of a pterocarpan fragment (II) (Fig. S2, Supplementary data).

The ^{13}C NMR spectrum revealed the presence of 55 carbon atoms: 15 atoms constituted the pterocarpan skeleton (lower moiety, II), 14 carbon atoms formed the 2-arylbezofuran fragment (upper moiety, I), 25 atoms belonged to the 2 geranyl side chains and 1 isoprenyl side chain, and 1 carbon atom belonged to the carbonyl group. The presence of the pterocarpan fragment (II) in **8** was confirmed by proton signals at δ_H 3.45 (1H, m), 3.57 (1H, m), 3.99 (1H, m), and 5.57 (1H, d, $J = 7.3$), assigned to H-6a, two H-6, and H-11a of the lower moiety (II), respectively. The chemical shift values of these signals were very similar to the signals of H-6a, two H-6, and H-11a protons in the ^1H spectrum of compounds **2–6** [15] and previously published lespebicolin A [14]. In the ^1H spectrum of **8**,we observed a singlet signal at δ_H 7.34 assigned to the aromatic proton H-7 (lower moiety, II) and two singlet signals of H-1 and H-4b of the pterocarpan fragment (lower moiety, II) at δ_H 7.21 (1H, s) and 6.36 (1H, s), respectively. A singlet signal at δ_H 6.81 (1H, s) was assigned to the aromatic proton H-5 of the 2-arylbezofuran fragment (upper moiety, I). The signals of the ABX proton system in the 2-arylbezofuran fragment at δ_H 6.50 (1H, d, $J = 2.4$), 6.41 (1H, dd, $J = 2.4, 8.4$), and 7.25 (1H, d, $J = 8.4$) belonged to H-3′, H-5′, and H-6′ protons of the 2-arylbezofuran moiety (upper moiety, I), respectively. The geranyl side chain was located at C-8 of the 2-arylbezofuran fragment (upper moiety, I), which was proven by the presence of the HMBC correlation between the signals of 2H-1″ at δ_H H 3.69 (2H, d, $J = 7.4$) and the signals of C-7, C-8 and C-9 (upper moiety, I) at δ_C 147.4, 111.0, and 141.9, respectively. The chemical shift values of the other atoms of the 2-arylbezofuran fragment (upper moiety, I) in the ^1H and ^{13}C NMR spectra closely resembled those for lespecyrtin H_2 [35] and lespebicolin A [14]. The structures of lespebicolin A and compound **8** differed only by the presence in **8** of an additional isoprenyl side chain attached to C-2 of the pterocarpan fragment (lower moiety, II), which was confirmed by HMBC correlations between H-1‴"at δ_H 3.33 (2H, m) and C-1, C-2, and C-3 at δ_C 132.0, 121.5, and 155.9 (lower moiety, II), respectively. The other geranyl side chain was attached to C-10 of the pterocarpan moiety (lower moiety, II), which was confirmed by the presence of HMBC correlations between the signal of 2H at δ_H 3.32 and the carbon signals of C-9, C-10, and C-10a at δ_C C 164.8, 112.1, and 164.9 (lower moiety, II), respectively.

We observed a cross-peak between the proton signal of H-7 at δ_H 7.34 (1H, s) of the pterocarpan fragment (lower moiety, II) and the carbon signal of C-4 (upper moiety, I) of the carbonyl group at δ_C 194.5 in the HMBC spectrum of **8**. Thus, we concluded that the carbonyl group was attached to C-8 of a pterocarpan fragment (lower moiety, II). The signal of the hydroxy group proton at C-9 of the pterocarpan fragment (lower moiety, II) had a δ_H of 12.82, which also confirmed that the carbonyl group was located at C-8 (lower moiety, II) and formed a hydrogen bond with this hydroxyl group. The signals in the ^1H and ^{13}C NMR spectra of **8** were assigned using HSQC, HMBC, and ROESY experiments (Figs. S5–S42, Supplementary data). Thus, compound **8**, named

Table 2
Anti-HSV-1 activity of polyphenolics from *L. bicolor* stem bark.

Compounds	CC_{50} (μM)	Pretreatment of virus		Pretreatment of cells		Simultaneous treatment		Treatment of infected cells	
		IC_{50} (μM)	SI	IC_{50} (μM)	SI	IC_{50} (μM)	SI	IC_{50} (μM)	SI
1	96.5 ± 13.5	10.5 ± 1.3	9.2 ± 1.0	57.4 ± 8.0	1.7 ± 0.2	20.3 ± 2.6	4.7 ± 0.6	26.8 ± 3.5	3.6 ± 0.4
2	72.8 ± 8.0	3.7 ± 0.4	19.7 ± 2.4	52.4 ± 7.3	1.4 ± 0.2	13.5 ± 0.5	5.4 ± 0.7	40.7 ± 5.7	1.8 ± 0.2
3	85.1 ± 11.1	26.6 ± 3.7	3.2 ± 0.4	>50	<2.0	>50	<2.0	>50	<2.0
4	72.6 ± 7.9	2.6 ± 0.3	28.0 ± 3.6	24.2 ± 3.1	3.0 ± 0.5	5.8 ± 0.7	12.5 ± 1.6	43.5 ± 6.1	1.7 ± 0.2
5	108.9 ± 13.1	9.7 ± 1.3	11.2 ± 1.2	>100	<1.0	16.0 ± 1.9	6.8 ± 0.9	>100	<1.0
6	63.0 ± 8.2	30.8 ± 4.0	2.0 ± 0.2	>50	<1.0	34.6 ± 4.5	1.8 ± 0.3	30.0 ± 4.5	2.1 ± 0.3
7	83.5 ± 9.2	>50	<2.0	>50	<2.0	17.8 ± 2.4	4.7 ± 0.5	44.2 ± 5.7	1.9 ± 0.2
8	>200	>50	<4.0	93.2 ± 13.0	2.1 ± 0.3	>50	<4.0	78.0 ± 10.1	2.6 ± 0.4
Acyclovir	>4000	NA		NA		9.3 ± 1.3	>430	0.4 ± 0.05	10,000

Note: Values are given as the means ± standard deviations of three or more independent experiments. Acyclovir® was used as the positive control. SI = CC_{50}/IC_{50}; NA–no activity.

Table 3
Anti-HSV-1 action of polyphenolics from *Lespedeza bicolor* flowers.

Compounds	CC_{50}	Pretreatment of virus		Pretreatment of cells		Simultaneous treatment		Treatment of infected cells	
		IC_{50}	SI	IC_{50}	SI	IC_{50}	SI	IC_{50}	SI
9	107.7 ± 14.0	8.6 ± 1.1	12.5 ± 1.6	>100	<1.0	21.9 ± 3.1	4.9 ± 0.6	>100	<1.0
11	177.8 ± 23.1	12.2 ± 1.5	14.6 ± 1.6	>100	<1.0	19.6 ± 2.5	9.1 ± 1.1	>100	<1.0
10 + 12	353.6 ± 38.8	3.6 ± 0.5	98.2 ± 11.8	>100	<1.0	2.4 ± 0.3	147 ± 20.6	98.0 ± 12.7	3.6 ± 0.4
Quercetin	268.4 ± 35.0	11.2 ± 1.4	24.0 ± 3.1	>100	<1.0	61.7 ± 8.0	4.4 ± 0.6	134.5 ± 18.8	2.0 ± 0.3

Note: Values are given as the means ± standard deviations of three or more independent experiments. Acyclovir® was used as the positive control. SI = CC_{50}/IC_{50}; NA–no activity.

Table 4
Description of the molecular descriptors used for QSAR model generation for the virucidal activity of polyphenolic compounds against HSV-1.

Class	Code	Description
i3D	vsurf_D1	Hydrophobic volume at −0.2
i3D	vsurf_D2	Hydrophobic volume at −0.4
i3D	vsurf_D6	Hydrophobic volume at −1.2
2D	SlogP_VSA9	Log of the octanol/water partition coefficient (including implicit hydrogens). This property is an atomic contribution model that calculates logP from the given structure, i.e., the correct protonation state). Sum of v_i such that $L_i > 0.40$.
2D	pmi	Principal moment of inertia.
2D	vsa_hyd	Approximation to the sum of VDW (Van der Waals) surface areas of hydrophobic atoms (Å2).
2D	vdw_area	Area of van der Waals surface ($Å^2$) calculated using a connection table approximation.

lespebicolin B, was assumed to be a dimeric flavonoid consisting of 2-arylbenzofuran and pterocarpan fragments linked via a carbonyl group, similar to lespebicolin A [14].

The absolute configuration of asymmetric centers at C-6a and C-11a in **8** was determined using the CD spectroscopy technique. We observed the following Cotton effects in the CD spectrum of **8**: λ_{max} (θ) 198 (+28,977), 214 (−45,398), 236 (−19,273), 272 (−5187), 300 (−3947), 340 (−8925), 395 (+1841). This CD spectrum closely resembled those of lespebicolin A [λ_{max} (θ) 198 (+40,706), 211 (−37,771), 235 (−33,085), 257 (+1494), 271 (−7833), 294 (−7058), 329 (−10,749), 392 (+3822)] [14] and lespecyrtin H_2 [λ_{max} (θ) 235 (−31,426), 270 (−13,232), 329 (−12,239), 340 (+860) [35], which had 6a*R*,11a*R* absolute configurations (Fig. S45 and S46, Supplementary data). The 6a*R*,11a*R* configuration of **8** was also confirmed by the negative optical rotation value ($[\alpha]^{20}_{Na/Hal}$ – 99).

The biosynthetic origin of dimeric flavonoids like lespebicolin B (**8**) is still an usettled issue. The linking carbon could derive from the 2-arylbenzofuran or, alternatively, from the pterocarpan moiety [36]. For lespebicolin B (**8**), the bridging carbon (carbonyl group) seemingly originates from a 2-aryl-benzofuran bearing extra carbon functionality at C-3 (formyl, hydroxymethyl, or methyl group [36] since compounds of this type were isolated from *L. bicolor* [16].

We also managed to isolate previously known 3-*O*-rutinosides of quercetin (**9**) and kaempferol (**11**), as well a mixture of 3-*O*-β-D-glucosides of quercetin and kaempferol (**10**,**12**) (2:1), from flowers of *L. bicolor*. The structural identification of 3-*O*-rutinosides of quercetin (**9**) and kaempferol (**11**) was performed by comparison of their ^1H and ^{13}C NMR spectra and HR-ESI-MS data with previously published data [37,38]. 3-*O*-β-D-glucosides of quercetin and kaempferol (**10**, **12**) were identified in the mixture by comparison of their HPLC-PDA-HR-ESI-MS profiles with those of standard samples purchased from Sigma-Aldrich.

3.2. Cytotoxic and ani-HSV-1 activity of polyphenolic compounds

A study of the cytotoxicity of polyphenolic compounds from *L. bicolor* against Vero cells was carried out using MTT assay. The results demonstrated that the cytotoxic activity of polyphenolics **1–8** did not differ significantly (Table 2). Their average 50% cytotoxic concentration (CC_{50}) value was approximately 85 μM; although, the CC_{50} of **8** was above 200 μM. The flavonoid glycosides from *L. bicolor* flowers showed low cytotoxicity, with CC_{50} values ranging from 107.7 to 353.6 μM. To further study the anti-HSV-1 effect of the tested compounds, concentrations of polyphenolics less than their CC_{50} values were used.

The antiviral effect of polyphenolic compounds from *L. bicolor* against HSV-1was assessed using the cytopathic effect (CPE) inhibition assay. To study the inhibitory effect of the tested compounds on different stages of virus replication, the polyphenols were added 1) to cells before infection (pretreatment of cells); 2) directly to the virus suspension (pretreatment of virus, virucidal activity); 3) to cells simultaneously with the virus (simultaneous treatment); and 4) after penetration of the virus into the host cells (treatment of infected cells).

We found that HSV-1 infection was suppressed most effectively when the virus was treated with polyphenolics directly but not when the tested compounds were added to the cells before the virus was absorbed or after it had entered the cell.

Pretreatment of HSV-1 with polyphenolic compounds (direct virucidal effect) showed that compounds **1**, **2**, **4**, and **5** significantly inhibited viral replication with SI ≥10 (Table 2). Compound **4** showed the highest efficiency among compounds **1**–**8**, with SI of 28.0, which may be due to the presence of an additional isoprenyl side chain in this compound. Compounds **9** and **11**, as well as the mixture of quercetin and kaempferol 3-*O*-β-D-glycosides (**10** and **12**), also showed significant virucidal activity with SI values of 12.5, 14.6, and 98.2, respectively (IC_{50} = 8.6, 12.2, and 3.6, respectively) (Table 3), whereas acyclovir showed no activity in this scheme. Usually, compounds with SI values higher than 10 are considered to be good therapeutic candidates and would potentially be effective and safe in the treatment of viral infection in vivo [39]. We should also note that lespebicolin B (**8**) did not show significant virucidal activity, which may be due to the fact that this compound is too bulky compared to compounds **1**–**7** to interact with virus proteins.

Treatment of Vero cells with polyphenolics **1–12** prior to HSV-1 infection (prophylactic effect) or to infected Vero cells 1 h after infection had no effect on viral replication acyclovir (SI of ~2 vs. 10,000). When the tested compounds and HSV-1 were added to Vero cells simultaneously to study their effect on the early stages of viral infection, we observed moderate antiviral activity of the tested polyphenolic compounds (SI of ~4.5), with (6a*R*,11a*R*)-2-isoprenyllespedezol A_2 (**4**) being the most active prenylated pterocarpan among the tested compounds with an SI of 12.5. The mixture of quercetin and kaempferol 3-*O*-β-D-gluicosides (**10** and **12**) demonstrated a good SI value of 147.0, but this was due to the high CC_{50} value (Table 3).

Notably, quercetin 3-*O*-rutinoside (rutin), kaempferol 3-*O*-rutinoside, and kaempferol 3-*O*-robinobioside were previously shown to be highly effective against HSV-1, reaching an SI of 266, 100, and 666, respectively, while the SI of their aglycons, quercetin, and kaempferol amounted to only 7.1 and 3.2, respectively. Kaempferol 3-*O*-robinobioside showed a similar SI value to that of acyclovir, the standard anti-HSV drug [40]. The anti-HSV-1 effects of quercetin were shown to be related to the suppression of TLR-3-dependent inflammatory

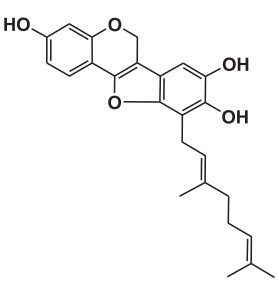

1

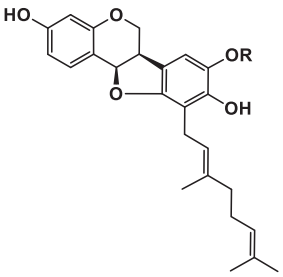

2 R = H

3 R = CH_3

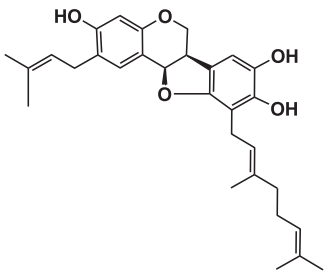

4

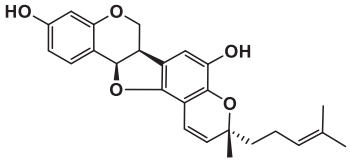

5

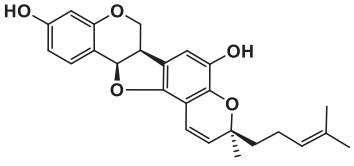

6

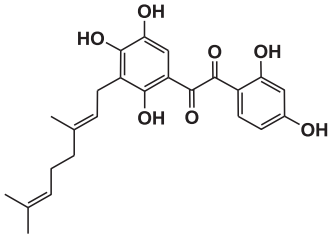

7

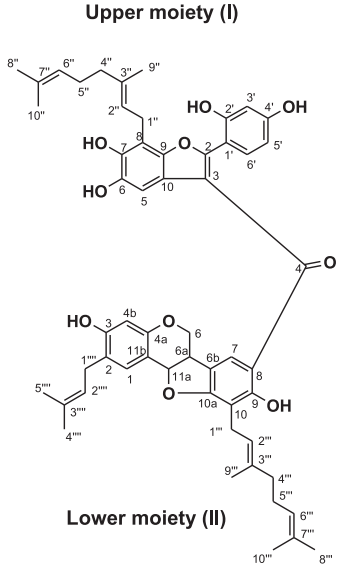

8 Lespebicolin B

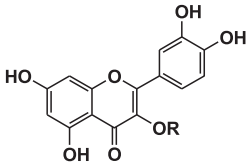

9R = α-L-Rha-(1→6)-β-D-Glu

10 R = β-D-Glu

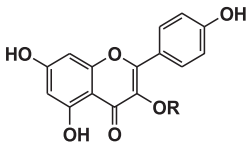

11R = α-L-Rha-(1→6)-β-D-Glu

12 R = β-D-Glu

Fig. 1. Structures of polyphenolic compounds isolated from *L. bicolor* stem bark and flowers.

responses in Raw 264.7 cells [41].

3.3. Computer modeling and QSAR analysis

A QSAR analysis was performed on a data set of 9 compounds possessing virucidal activity with 4 < pIC_{50} < 6. The descriptors were calculated using the MOE QuaSAR-Model module for compounds in the data sets. The calculated descriptors were initially screened using the QuaSAR-Contingency module of MOE, which is a statistical application designed to assist in the selection of descriptors for QSAR. The QuaSAR-Model module in MOE was used to generate the QSAR models with the partial least square (PLS) method. An analysis of the models using the QuaSAR-Model report made it possible to select a smaller number of the most important molecular descriptors and to obtain models with a smaller number of descriptors. The descriptors having an effect on the performance of prediction of polyphenol virucidal activity with QSAR models and used for QSAR model generation are described in Table 4.

The QSAR models were constructed based on the 7 selected molecular descriptors using the QuaSAR-Model module in MOE 2020.0901. The regression analysis of the QuaSAR-Model was used to build the QSAR model using PLS for the 9 compounds with a correlation coefficient (R2) of 0.98787 and an RMSE (root mean square error) of 0.03312 (Table 5, Fig. 2). The obtained model was validated using cross-validation leave-one-out (LOO). The best QSAR model established using a data set consisting of 9 polyphenols was as follows:

pIC_{50}
12.39179
–0.00704 * vsurf_D2
+0.02301 * vsurf_D6
–0.01020 * vsurf_D1
+0.01049 * vsa_hyd
–0.02770 * vdw_area
+0.00100 * pmi
–0.01313 * SlogP_VSA9

An analysis of the relative importance of the QSAR model descriptors showed that the most important descriptors were the 2D descriptor principal moment of inertia (pmi) and the i3D descriptor vsurf_D1 (hydrophobic volume at −0.2) (Fig. 3).

It was found that the virucidal activity of polyphenolics depends on both the structure of the cyclic part of the molecules (Fig. 4A) and the conformation of the geranyl side chains (Fig. 4B). This correlates with the largest value of the pmi descriptor describing the geometry of the molecules (Fig. 4). We observed good correlation between the experimental data and the predicted virucidal activity of prenylated pterocarpans and flavonoid glycosides ($R = 0.9879$).

4. Conclusion

It has been shown that prenylated pterocarpans from *L. bicolor* possess direct virucidal activity. (6a*R*,11a*R*)-2-Isoprenyllespedezol A_2 (**4**) was the most effective among the tested compounds. Rutinosides of quercetin and kaempferol and the mixture of glucosides of quercetin and kaempferol (**10** and **12**) also showed significant virucidal active. However, the plyphenolic compounds from *L. bicolor* were not effective under pretreatment of cells or treatment of infected cellswith

Table 5
Comparison of the experimental pIC_{50} values of the virucidal activity of polyphenolic compounds and the predicted activity (PRED pIC_{50}) values according to QSAR model.

Compound	pIC_{50}	PRED pIC_{50}	RES[a]
1	4.9590	4.9358	0.02315
2	5.4320	5.4322	−0.00021
4	5.5850	5.6097	−0.02476
5	5.0130	4.9589	0.05408
6	4.5850	4.6235	−0.03854
9	5.0659	5.0204	0.04550
10	5.4439	5.4416	0.00238
11	4.9140	4.9578	−0.04384
Qurcetin	4.9510	4.9687	−0.01775

[a] RES = pIC_{50} − PRED pIC_{50}.

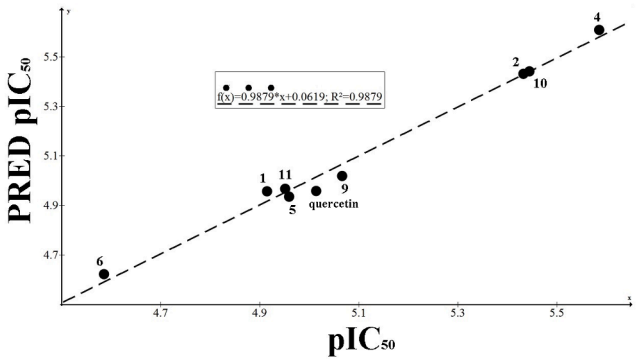

Fig. 2. Predicted virucidal activity of polyphenolic compounds as a function of experimental values of virucidal activity of polyphenolic compounds for HSV-1.

Fig. 2. Predicted virucidal activity of polyphenolic compounds as a function of experimental values of virucidal activity of polyphenolic compounds for HSV-1.

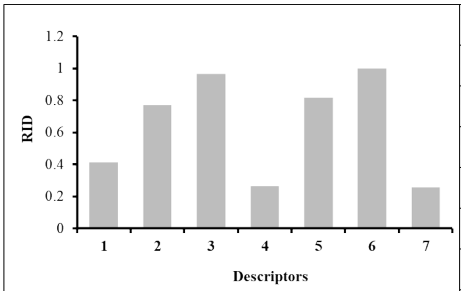

N	Descriptor	RID
1	vsurf_D2	0.4124
2	vsurf_D6	0.7690
3	vsurf_D1	0.9632
4	vsa_hyd	0.2635
5	vdw_area	0.8150
6	pmi	1.000
7	SlogP_VSA9	0.2568

Fig. 3. The relative importance of descriptors (RID) used for the QSAR model of virucidal activity of polyphenolic compounds.

Fig. 3. The relative importance of descriptors (RID) used for the QSAR model of virucidal activity of polyphenolic compounds.

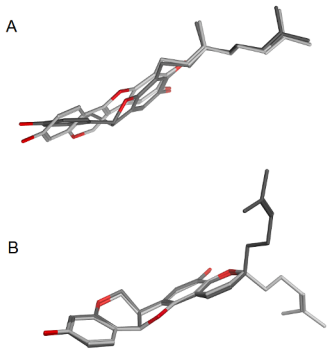

Fig. 4. Superposition of 3D structures of compounds **1** and **2** (A) and **5** and **6** (B). Structures **1** and **5** are shown in light gray, and structures **2** and **6** are shown in dark gray.

Fig. 4. Superposition of 3D structures of compounds **1** and **2** (A) and **5** and **6** (B). Structures **1** and **5** are shown in light gray, and structures **2** and **6** are shown in dark gray.

polyphenolics.

QSAR analysis confirmed that the virucidal activity of polyphenolic compounds from *L. bicolor* depends on both the structure of the aromatic part and the conformation of geranyl and isoprenyl side chains of their molecules. The experimental data correlated well enough with the predicted virucidal activity of prenylated pterocarpans and flavonoid glycosides ($R = 0.9879$).

Credit author statement

Darya V. Tarbeeva Sergey A. Fedoreyev – isolation and structure elucidation of polyphenolic compounds from *L. bicolor*.

Natalya V. Krylova, Olga V. Iunikhina, Mikhail Yu. Shchelkanov – investigated antiviral activity of polyphenolic compounds.

Galina N. Likhatskaya - performed QSAR analysis.

Anatoliy I. Kalinovskiy – recorded NMR spectra.

Valeria P. Grigorchuk – recorded HR-MS spectra.

Declaration of interest

The authors declare that they have no known competing financial interests or personal relationships that could have appeared to influence the work reported in this paper.

Appendix A. Supplementary data

Supplementary data to this article can be found online at https://doi.org/10.1016/j.fitote.2021.105121.

References

[1] S.C. Park, N.R. Rim, N.W. Kim, Antioxidative activity and irritation response of *Lespedeza bicolor*, J. Toxicol. Public Health 21 (2005) 115–119, https://doi.org/10.9721/KJFST.2020.52.1.26.

[2] S.J. Lee, M.D. Hossaine, S.C. Park, A potential anti-inflammation activity and depigmentation effect of *Lespedeza bicolor* extract and its fractions, Saudi J. Biol. Sci. 23 (1) (2016) 9–14, https://doi.org/10.1016/j.sjbs.2015.01.016.

[3] H.H. Yoo, T. Kim, S. Ahn, Y.J. Kim, H.Y. Kim, X.L. Piao, J.H. Park, Evaluation of the estrogenic activity of Leguminosae plants, Biol. Pharm. Bull. 28 (3) (2005) 538–540, https://doi.org/10.1248/bpb.28.538.

[4] A. Samiullah, R. Bano, H. Naz, Yasmin, *In vitro* inhibition potential of *Lespedeza bicolor* Turcz against selected bacterial and fungal strains, J. Med. Plant Res. 5 (16) (2011) 3708–3714.

[5] S. Ullah, Methanolic extract from *Lespedeza bicolor*: potential candidates for natural antioxidant and anticancer agent, J. Tradit. Chin. Med. 37 (4) (2017) 444–451.

[6] S.Y. Ha, J.Y. Jung, H.Y. Kang, T.H. Kim, J.K. Yang, Tyrosinase activity and melanogenic effects of *Lespedeza bicolor* extract *in vitro* and *in vivo*, Bioresources 15 (2020) 6244–6261, https://doi.org/10.15376/biores.15.3.6244–6261.

[7] M.H. Do, J.H. Lee, H.M. Wahedi, C. Pak, C.H. Lee, E.J. Yeo, Y. Lim, S.K. Ha, I. Choi, S.Y. Kim, *Lespedeza bicolor* ameliorates endothelial dysfunction induced by methylglyoxal glucotoxicity, Phytomedicine 36 (2017) 26–36, https://doi.org/10.1016/j.phymed.2017.09.005.

[8] M.H. Do, J.-S. Lee, K. Cho, M.C. Kang, L. Subedi, A. Parveen, S.Y. Kim, Therapeutic potential of *Lespedeza bicolor* to prevent methylglyoxal-induced glucotoxicity in familiar diabetic nephropathy, J. Clin. Med. 8 (8) (2019) 1138, https://doi.org/10.3390/jcm8081138.

[9] Y. Kim, H. Lee, S.Y. Kim, Y. Lim, Effects of *Lespedeza bicolor* extract on regulation of AMPK associated hepatic lipid metabolism in type 2 diabetic mice, Antioxidants 8 (12) (2019) 599, https://doi.org/10.3390/antiox8120599.

[10] Y.H. Ko, K.Y. Shim, S.K. Kim, J.Y. Seo, B.R. Lee, K.H. Hur, Y.J. Kim, S.E. Kim, M. H. Do, A. Parveen, S.Y. Kim, S.Y. Lee, C.G. Jang, *Lespedeza bicolor* extract improves amyloid Beta 25–35-induced memory impairments by upregulating BDNF and activating Akt, ERK, and CREB signaling in mice, Planta Med. 85 (17) (2019) 1363–1373, https://doi.org/10.1055/a-1018-5402.

[11] V.I. Glyzin, A.I. Bankovskii, O.V. Zhurba, V.I. Sheichenko, Flavonoids of *Lespedeza bicolor*, Chem. Nat. Compd. 6 (4) (1970) 473–474.

[12] J.H. Lee, J.W. Jhoo, Antioxidant activity of different parts of Lespedeza bicolor and isolation of antioxidant compound, Korean J. Food Sci. Technol. 44 (6) (2012) 763–771.

[13] H.S. Woo, D.W. Kim, M.J. Curtis-Long, B.W. Lee, J.H. Lee, J.Y. Kim, J.E. Kang, K. H. Park, Potent inhibition of bacterial neuraminidase activity by pterocarpans isolated from the roots of *Lespedeza bicolor*, Bioorg. Med. Chem. Lett. 21 (20) (2011) 6100–6103.

[14] S.A. Dyshlovoy, D.V. Tarbeeva, S.A. Fedoreyev, T. Busenbender, M. Kaune, M. V. Veselova, A.I. Kalinovskiy, J. Hauschild, V.P. Grigorchuk, N.Y. Kim, C. Bokemeyer, M. Graefen, P.G. Gorovoy, Gunhild von Amsberg, Polyphenolic compounds from *Lespedeza bicolor* root bark inhibit progression of human prostate cancer cells via induction of apoptosis and cell cycle arrest, Biomolecules 10 (3) (2020) 451, https://doi.org/10.3390/biom10030451.

[15] D.V. Tarbeeva, S.A. Fedoreyev, M.V. Veselova, A.S. Blagodatski, A.M. Klimenko, A. I. Kalinovskiy, V.P. Grigorchuk, D.V. Berdyshev, P.G. Gorovoy, Cytotoxic polyphenolic compounds from *Lespedeza bicolor* stem bark, Fitoterapia 135 (2019) 64–72, https://doi.org/10.1016/j.fitote.2019.04.003.

[16] N.T.T. Thuy, J.E. Lee, H.M. Yoo, N. Cho, Antiproliferative pterocarpans and coumestans from *Lespedeza bicolor*, J. Nat. Prod. 82 (11) (2019) 3025–3032, https://doi.org/10.1021/acs.jnatprod.9b00567.

[17] J.-E. Lee, F. Bo, N.T.T. Thuy, J. Hong, J.S. Lee, N. Cho, H.M. Yoo, Anticancer activity of lesbicoumestan in Jurkat cells via inhibition of oxidative stress-mediated apoptosis and MALT1 protease molecules, Molecules 26 (1) (2021) 185, https://doi.org/10.3390/molecules26010185.

[18] K.J. Looker, A.S. Magaret, M.T. May, K.M. Turner, P. Vickerman, S.L. Gottlieb, L. M. Newman, Global and regional estimates of prevalent and incident herpes simplex virus type 1 infections in 2012, PloSOne 10 (2015), https://doi.org/10.1371/journal.pone.0140765 e0140765 [1–17].

[19] A. Subramaniam, W.J. Britt, Herpes viridae infection: prevention, screening, and management, Clin. Obstet. Gynecol. 61 (1) (2018) 157–176, https://doi.org/10.1097/GRF.0000000000000335.

[20] J.B. Suzich, A.R. Cliffe, Strength in diversity: understanding the pathways to herpes simplex virus reactivation, Virology 522 (2018) 81–91, https://doi.org/10.1016/j.virol.2018.07.011.

[21] WHO, Herpes simplex virus, News bulletin 400 (2016). www.who.int/mediacentre/factsheets/fs400/ru.

[22] Online WHO Coronavirus (COVID-19) Dashboard. World Health Organization. https://covid19.who.int. Accessed April 24, 2021.

[23] K. Klysik, A. Pietraszek, A. Karewicz, M. Nowakowska, Acyclovir in the treatment of herpes viruses – a review, Curr. Med. Chem. 27 (24) (2020) 4118–4137, https://doi.org/10.2174/0929867325666180309105519.

[24] J. Piret, G. Boivin, Resistance of herpes simplex viruses to nucleoside analogues: mechanisms, prevalence, and management, Antimicrob. Agents Chemother. 55 (2) (2011) 459–472, https://doi.org/10.1128/AAC.00615-10.

[25] Y.-C. Jiang, H. Feng, Y.-C. Lin, X.-R. Guo, New strategies against drug resistance to herpes simplex virus, Int. J. Oral Sci. 8 (1) (2016) 1–6, https://doi.org/10.1038/ijos.2016.3.

[26] D. Pan, S.B. Kaye, M. Hopkins, R. Kirwan, I.J. Hart, D.M. Coen, Common and new acyclovir resistant herpes simplex virus-1 mutants causing bilateral recurrent herpetic keratitis in an immunocompetent patient, J. Infect. Dis. 209 (3) (2014) 345–349, https://doi.org/10.1093/infdis/jit437.

[27] L.D. Turner, P. Beckingsale, Acyclovir-resistant herpetic keratitis in a solid-organ transplant recipient on systemic immunosuppression, Clin. Ophthalmol. 7 (2013) 229–232, https://doi.org/10.2147/OPTH.S39113.

[28] S. Lalani, C.L. Poh, Flavonoids as antiviral agents for enterovirus A71 (EV-A71), Viruses 12 (2) (2020) 184, https://doi.org/10.3390/v12020184.

[29] X. Chen, H. Qiao, T. Liu, Z. Yang, L. Xu, Y. Xu, H.M. Ge, R.-X. Tan, E. Li, Inhibition of herpes simplex virus infection by oligomeric stilbenoids through ROS generation, Antivir. Res. 95 (1) (2012) 30–36, https://doi.org/10.1016/j.antiviral.2012.05.001.

[30] T. Mosmann, Rapid colorimetric assay for cellular growth and survival: application to proliferation and cytotoxicity assays, J. Immunol. Methods 65 (1–2) (1983) 55–63, https://doi.org/10.1016/0022-1759(83)90303-4.

[31] O.S. Weislow, R. Kiser, D.L. Fine, J. Bader, R.H. Shoemaker, M.R. Boyd, New soluble-formazan assay for HIV-1 cytopathic effects: application to high-flux screening of synthetic and natural products for AIDS-antiviral activity, J. Natl. Cancer Inst. 81 (1989) 577–586, https://doi.org/10.1093/jnci/81.8.577.

[32] L.J. Reed, H. Muench, A simple method of estimating fifty percent's endpoints, Am. J. Hyg. 27 (1938) 493–497.

[33] A. Astani, P. Schnitzler, Antiviral activity of monoterpenes beta-pinene and limonene against herpes simplexvirus *in vitro*, Iran J. Microbiol. 6 (3) (2014) 149–155.

[34] Molecular Operating Environment (MOE), 2020.09; Chemical Computing Group ULC, 1010 Sherbrooke St. West, Suite #910, 2020. Montreal, QC, Canada, H3A 2R7.

[35] M. Mori-Hongo, H. Yamaguchi, T. Warashina, T. Miyase, Melanin synthesis inhibitors from *Lespedeza cyrtobotrya*, J. Nat. Prod. 72 (1) (2009) 63–71.

[36] N.C. Veitch, Isoflavonoids of the leguminosae, Nat. Prod. Rep. 30 (2013) 988–1027.

[37] G. Yoo, S.J. Park, T.H. Lee, H. Yang, Y. Baek, N. Kim, Y.J. Kim, S.H. Kim, Flavonoids isolated from *Lespedeza cuneata* G. Don and their inhibitory effects on nitric oxide production in lipopolysaccharide-stimulated BV-2 microglia cells, Pharmacogn. Mag. 11 (43) (2015) 651–656, https://doi.org/10.4103/0973-1296.160466.

[38] M. Olszewska, Flavonoids from *Prunus serotina* Ehrh, Acta Pol. Pharm. 62 (2) (2005) 127–133.

[39] G. Indrayanto, G.S. Putra, F. Suhud, Validation of *in-vitro* bioassay methods: application in herbal drug research, Profiles Drug Subst. Excip. Relat. Methodol. 46 (2021) 273–307, https://doi.org/10.1016/bs.podrm.2020.07.005.

[40] L. Yarmolinsky, M. Huleihel, M. Zaccai, S. Ben-Shabat, Potent antiviral flavone glycosides from *Ficus benjamina* leaves, Fitoterapia 83 (2012) 362–367, https://doi.org/10.1016/j.fitote.2011.11.014.

[41] S. Lee, H.H. Lee, Y.S. Shin, H. Kang, H. Cho, The anti-HSV-1 effect of quercetin is dependent on the suppression of TLR-3 in Raw 264.7 cells, Arch. Pharm. Res. 40 (5) (2017) 623–630, https://doi.org/10.1007/s12272-017-0898-x.